

Continuous Prompts: LLM-Augmented Pipeline Processing over Unstructured Streams

Shu Chen
Brown University
Providence, USA
shu_chen@brown.edu

Deepti Raghavan
Brown University
Providence, USA
deeptir@brown.edu

Uğur Çetintemel
Brown University
Providence, USA
ugur_cetintemel@brown.edu

ABSTRACT

Monitoring unstructured streams increasingly requires persistent, semantics-aware computation, yet today’s LLM frameworks remain stateless and one-shot, limiting their usefulness for long-running analytics. We introduce *Continuous Prompts* (CPs), the first framework that brings LLM reasoning into continuous stream processing. CPs extend RAG to streaming settings, define continuous semantic operators, and provide multiple implementations, primarily focusing on LLM-based approaches but also reporting one embedding-based variants. Furthermore, we study two LLM-centric optimizations, tuple batching and operator fusion, to significantly improve efficiency while managing accuracy loss.

Because these optimizations inherently trade accuracy for speed, we present a dynamic optimization framework that uses lightweight *shadow executions* and cost-aware *multi-objective Bayesian optimization* (MOBO) to learn throughput–accuracy frontiers and adapt plans under probing budgets.

We implement CPs in the VectraFlow stream processing system. Using operator-level microbenchmarks and streaming pipelines on real datasets, we show that VectraFlow can adapt to workload dynamics, navigate accuracy–efficiency trade-offs, and sustain persistent semantic queries over evolving unstructured streams.

1 INTRODUCTION

Large language models (LLMs) have become the de-facto tool for interpreting diverse unstructured data, from text and images to tables and semi-structured documents. Yet most LLM pipelines today are stateless and episodic: they evaluate isolated prompts over static corpora, with limited support for operator state, persistence, or long-running adaptivity. Many emerging applications (e.g., clinical monitoring, financial surveillance, regulatory compliance) have fundamentally different needs: they require continuous, semantics-aware computation over evolving data streams, often under resource budgets that force explicit performance–accuracy trade-offs.

We argue that supporting these workloads requires the LLM analog of data-stream processing systems. To this end, we introduce *Continuous Prompts* (CPs), which extend one-shot prompt execution into stateful, long-lived, and adaptive computations over unstructured streams. Just as continuous queries lift relational operators to unbounded data, CPs lift LLM semantics into continuous, pipeline-level operators. Building CPs requires: (i) LLM-native semantic operators with explicit state and composable semantics; (ii) continuous operator variants — windowing, grouping, and retrieval — that track evolving content rather than fixed windows; and (iii) runtime mechanisms that balance efficiency and accuracy under dynamic conditions.

Several recent systems (e.g., Palimpsest [12], Lotus [17], DocETL [19]) introduced semantic operators for LLM-based analytics, but they execute in batch or one-shot settings. They lack support for unbounded streams and provide no mechanisms for optimizing LLM execution as workloads shift or as accuracy–throughput trade-offs evolve. Our prior work [14] addresses streaming semantics by operating over embedding-based operators such as vector filters and vector topk, enabling continuous processing but only at the vector level. In contrast, the present work brings continuous processing to the LLM semantic layer, introducing continuous semantic operators, and adaptive optimization techniques tailored to the challenges of persistent LLM-based pipeline execution, which is our focus. Embedding-based implementations, explored extensively in VectraFlow and related systems, appear primarily as comparison points in the accuracy–throughput design space.

We implement CPs on VectraFlow [14], extending the system with LLM-based implementations of continuous semantic operators. In addition to leveraging established techniques such as embedding-based retrieval and indexing, we comprehensively investigate two new LLM-specific optimizations. *Tuple batching* groups multiple input tuples into a single LLM call to amortize invocation overhead, and *operator fusion* combines multiple semantic operators into a single prompt to reduce model invocations and exploit cross-operator structure. Both techniques introduce performance–accuracy trade-offs, which our system explicitly measures, models, and manages through dynamic planning.

At runtime, VectraFlow’s *dynamic optimization framework* unifies operator-level statistics and sensitivity profiles into a global execution planner that continuously balances performance and accuracy. The planner integrates offline operator-level microbenchmarks with live telemetry to generate, evaluate, and reconfigure execution plans on the fly. It explores fusible operator chains, adaptive batch sizes, and alternative implementations (e.g., embedding-based variants), ranking candidate plans using predictive cost–accuracy models. In summary, this paper makes the following contributions:

- We introduce *continuous prompts* (CPs)—the LLM counterpart of continuous queries—for stateful, adaptive processing of unstructured data streams, and extend prior semantic operator models to continuous settings with new constructs such as semantic windows, dynamic semantic group-by, and continuous RAG (Section 3).
- We study two LLM-centric execution optimizations, *tuple batching* and *operator fusion*, and quantify their performance–accuracy trade-offs through operator sensitivity profiles (Section 4).
- We design a dynamic optimization framework that integrates operator-level insights with cost models and online telemetry, enabling adaptive plan selection at run-time (Section 5).

- We propose a cost-aware multi-objective Bayesian optimization (MOBO) algorithm that efficiently learns accuracy–throughput trade-off curves and guides sample-efficient plan adjustments under probing budgets (Section 6).
- We implement these ideas in *VectraFlow* and demonstrate that it can effectively trade off performance and accuracy in response to changing workload conditions on realistic streaming pipelines (Section 7).

The rest of the paper is organized as follows. Section 2 introduces the VectraFlow architecture, system model, and general semantic operators. Section 3 presents our streaming-native semantic operators. Section 4 describes our execution-level optimizations and analyzes their throughput–accuracy trade-offs. Section 5 describes the dynamic planning framework, including its architecture and cost and accuracy models. Section 6 details our cost-aware MOBO algorithm for efficient frontier learning and adaptive plan selection. Section 7 reports the evaluation setup and results, including two end-to-end real-world streaming pipelines. Finally, Sections 8 and 9 review related work and conclude the paper.

2 VECTRAFLOW

2.1 System Model

The VectraFlow architecture [14] follows a traditional data-flow system model. It formalizes continuous semantic stream processing as a composition of stateful LLM-based operators over unstructured data streams.

Unstructured Streams. The system ingests unbounded streams of unstructured content such as clinical notes, financial news, or social media posts. These inputs are heterogeneous in length, style, and vocabulary, often lacking predefined schema or fixed attributes. The goal is to continuously interpret and transform such data into structured semantic representations.

Data Model. Incoming data are modeled as timestamped tuples $S = \{(t_i, x_i) \mid i = 1, 2, \dots\}$, where t_i denotes the arrival time and x_i is the tuple payload in an extended relational model, where tuples can contain both conventional structured attributes and one or more unstructured attributes (e.g., a document or message) that are fed to semantic operators. Each tuple is processed incrementally upon arrival, forming the atomic unit of streaming computation.

Operator Model. A query plan consists of a directed acyclic graph of *semantic operators* $O = \{o_1, \dots, o_k\}$. Each operator is realized by an LLM or embedding-based function that implements a continuous, stateful transformation such as semantic mapping, filtering, segmentation (windowing, group-by), or ranking (top- k). Operators maintain internal state $s_j(t)$ and update it as new tuples arrive, enabling the system to adapt to semantic drift in the stream.

Execution Model. Tuples are processed either individually or in mini-batches of size T to amortize LLM invocation overhead. Adjacent operators may be fused into a single invocation to further reduce redundant prefill costs. The system ensures order-preserving propagation across operators and continuous state updates.

Cost Model. Each operator execution is associated with a cost vector $C(o_j) = \langle \text{throughput}(o_j), \text{accuracy}(o_j) \rangle$, capturing processing efficiency in tuples per second and semantic fidelity. These

metrics form the foundation for dynamic plan optimization, guiding runtime adjustments of batch size, fusion strategy, and operator implementation.

2.2 General Semantic Operators

VectraFlow extends traditional relational data-flow models with a suite of LLM-driven semantic operators that process unstructured streams. Table 1 provides a complete overview of these operators. The general semantic operators are designed to apply uniformly in both batching and streaming execution modes. In particular, operators such as semantic top- k and semantic aggregate include incremental modes that maintain evolving state as new tuples arrive, enabling streaming-native execution.

3 STREAMING-NATIVE SEMANTIC OPERATORS

We introduce streaming-specific semantic operators that enable adaptive, LLM-driven processing over unstructured data. Specifically, we present three core operators and primarily LLM-based implementations and analyze their behavior through microbenchmarks using the same experimental setup as in *Experimental Setup* (§7.1). For completeness, we also evaluate embedding-based implementations when they provide a meaningful comparison.

3.1 Semantic Windows (ω_s)

Stream processing systems use *windows* as logical boundaries to segment data for incremental computation. Conventional approaches rely on time-based or count-based windows (e.g., “5-minute intervals” or “100-event batches”), but these static strategies often fail to align with evolving data semantics. To address this limitation, we propose *semantic windows*, which dynamically adjust their boundaries based on contextual meaning. By detecting signals such as topic shifts, sentiment changes, or new entity mentions, semantic windows can align execution with the intrinsic structure of the stream rather than with arbitrary temporal or cardinal triggers.

Our design leverages a semantic windowing mechanism that incrementally evaluates the semantic coherence of incoming tuples. The LLM assigns a *continuity score* to each new tuple, indicating whether it belongs to the current window or should trigger the start of a new one. Whenever this score falls below a threshold, reflecting shifts such as topic drift, entity transitions, or narrative changes, the operator can infer a semantic boundary. A typical evaluation prompt might be:

“Given the tuples in the current window, should the semantic window remain open? Analyze the tuples for key shifts such as <topic drift>, <new entity reference>, or <narrative change>. If one of these events occurs, return a continuity score from 0 to 1, where 1 indicates high continuity and 0 signals that a new window should start.”

Implementation. We explore three strategies for realizing semantic windowing: (1) *Pairwise Semantic Window*, which computes a continuity score $\text{cont}(x_t, x_{t-1})$ between consecutive tuples; when the score drops below a threshold τ , a new window is opened,

Table 1: Overview of continuous semantic operators in VectraFlow.

Operator	Description	Example Use Case
General Semantic Operators (batching & streaming)		
Semantic Filter (σ_s)	Applies an LLM-based predicate that returns a boolean decision for each tuple; tuples evaluated as <i>true</i> pass the filter, enabling semantic selection by topic, sentiment, or entity	Select tweets related to <i>Ukraine</i> or <i>COVID-19</i> from a mixed news stream.
Semantic Map (π_s)	Transforms unstructured text into structured records such as entities, relations, or JSON key–value pairs.	Extract company name and event from news headlines.
Semantic Aggregate (γ_s)	Computes summaries or trends over semantic windows; supports both standard and incremental modes via <code>init()</code> , <code>increment()</code> , and <code>finalize()</code> .	Continuously summarize market sentiment over the last 100 tweets mentioning Apple (\$AAPL).
Semantic Top-k (τ_s)	Maintains the k most relevant tuples using a continuous scoring function that evaluates impact, novelty, or topical importance.	Select the 10 most influential financial news items as the market evolves.
Semantic Join (\bowtie_s)	Correlates tuples across streams based on semantic similarity rather than strict key equality.	Match analyst reports to relevant stock price movements.
Streaming-Native Semantic Operators		
Semantic Window (ω_s)	Dynamically adjusts window boundaries based on topic or sentiment shifts to align computation with semantic changes.	Detect when discourse shifts from “peace talks” to “sanctions” in the Ukraine event stream.
Semantic Group-By (μ_s)	Groups tuples by meaning in streaming data, allowing categories to emerge, evolve, and dissolve over time.	Track evolving news events and continuously update group assignments as new information shifts the underlying topics.
Continuous RAG (ρ_s)	Maintains evolving prompts that continuously fetch relevant context as query scope shifts, enabling real-time retrieval from streams.	Continuously monitor the financial news articles that are relevant to my stock portfolio.

otherwise the current one is extended—this serves as our baseline; (2) *Summary-based Semantic Window*, which maintains multiple overlapping windows, each with an evolving summary S_i ; for each incoming tuple x_t , the system assigns it to the window with the highest continuity score $\text{cont}(x_t, S_i)$ above τ , updating the selected summary incrementally via incremental aggregation; and (3) *Embedding-based Semantic Window*, which maintains live clusters with representatives and assigns x_t to the most similar cluster if similarity $\geq \tau$, otherwise creating a new cluster. The threshold τ is tuned for the best observed performance.

Evaluation. We evaluate three semantic windowing strategies in Figure 1 using the MiDe22 [21] dataset, which consists of 40 temporally ordered events. The goal is to detect event shifts and assign tweets from the same ground-truth event to a common window. We construct *overlapping* windows with an expiry mechanism that retires fading topics gracefully and prevents repeated splits under gradual drift. We evaluate two dimensions: *event grouping* and *boundary detection*. For grouping, we report F1 and ARI: F1 reflects item-level precision and recall, while ARI captures pairwise agreement between predicted and true event partitions. For boundary detection, we use Boundary F1 and Purity: Boundary F1 measures how accurately transition points are identified, and Purity reflects the dominance of a single ground-truth event within each predicted window. High Purity indicates strong internal consistency but may also signal *over-segmentation*.

Takeaway. M3 (Embeddings) produces the most accurate boundaries, yielding the highest Boundary F1. M1 (Pairwise) achieves the highest Purity by capturing fine-grained drift, though at the cost

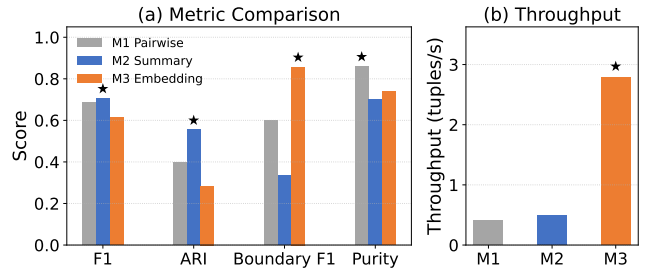


Figure 1: Semantic window implementations on the MiDe22 dataset. Left: metric comparison (F1, ARI, Boundary F1, and Purity), with \star indicating the best score. Right: throughput in tuples/s.

of over-segmentation. M2 (Summary) delivers the strongest event-grouping performance (F1 and ARI), maintaining long, coherent windows but with less precise boundary placement.

3.2 Semantic Group-By (μ_s)

We extend the conventional group-by abstraction to unstructured, continuously arriving data. Unlike key-based grouping over explicit attributes, *semantic group-by* clusters tuples by meaning, forming groups that share a coherent topic or event. While prior systems such as Lotus support offline semantic group-by over static corpora (e.g., grouping ArXiv papers into k topics), our setting requires clusters to evolve with the stream itself—topics drift, new entities appear, and old ones fade.

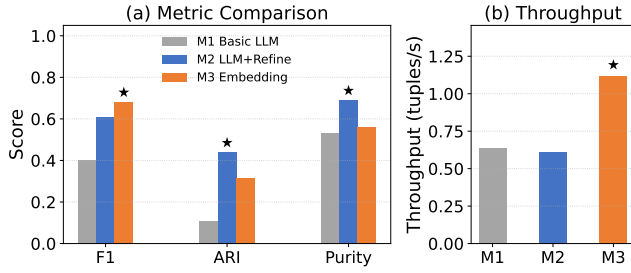


Figure 2: Semantic group-by implementations on the MiDe22 dataset. Left: metric comparison (F1, ARI, Boundary F1, and Purity), with ★ indicating the best score. Right: throughput in tuples/s.

We therefore introduce a **dynamic semantic group-by** operator that creates, refines, and retires categories on the fly, ensuring groups remain aligned with the current semantic landscape. The operator uses LLM-based comparisons or few-shot prompts to decide membership incrementally, with embedding-based grouping as a lighter alternative. For example, the operator tracks evolving news events—merging early reports on “peace talks” and “sanctions” into broader “Ukraine conflict” clusters as the story unfolds.

Implementation. Our dynamic semantic group-by design is informed by the incremental clustering [4] that update cluster representatives online as new data arrives. Building on these ideas, we implement three approaches: (1) *Basic LLM Group-By*, where each tuple is analyzed by the LLM and either assigned to an existing group or used to create a new one, maintaining a dictionary of group names and descriptions; this method is lightweight and fully adaptive but may produce redundant or noisy groups; (2) *LLM with Refinement Group-By*, which periodically revisits and restructures the grouping—merging, splitting, or renaming categories to better track topic drift, at the expense of additional LLM calls; and (3) *Embedding-based Group-By*, which embeds tuples into a vector space and performs incremental clustering, periodically sampling a small number of items from each cluster and invoking an LLM prompt to generate an updated, interpretable cluster name.

Evaluation. We compare the three approaches on a MiDe22 subset, reporting F1, ARI, Purity, and throughput (tuples/s) in Figure 2. The LLM with Refinement method periodically issues an additional refinement prompt every 10 tuples.

Takeaway. *Embedding-based* grouping is fast and achieves high item-level F1, but its over-segmentation produces fragmented events. *Basic LLM* offers moderate coherence and speed, while *LLM with Refinement* delivers the cleanest, most globally consistent clusters at a modest throughput cost, making it the best option when preserving event structure is the priority.

3.3 Continuous RAG

To support retrieval over evolving streams, we introduce *continuous RAG*, the continuous analog of traditional Retrieval-Augmented Generation (RAG). While traditional RAG performs data retrieval from a stored data store based on relevance to a one-time prompt, continuous RAG retrieves relevant data from input streams based on their relevance to a continuous prompt. More specifically, traditional RAG runs once: a fixed prompt retrieves relevant items from

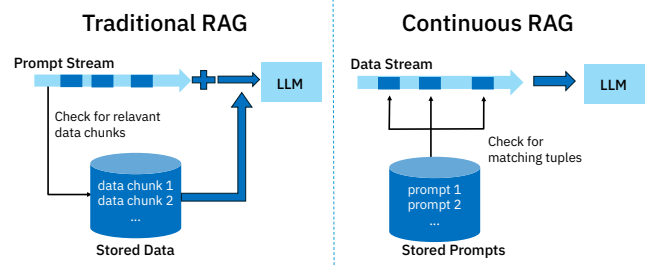


Figure 3: Traditional RAG vs. Continuous RAG.

a stored corpus, whereas continuous RAG operates continuously, using prompts to retrieve semantically relevant tuples from the live stream. Figure 3 contrasts traditional RAG’s static retrieval model with continuous RAG’s stream-oriented retrieval process.

Continuous RAG maintains a long-lived retrieval state that is incrementally updated as new tuples arrive. In practice, VectraFlow uses LLM-generated sub-prompts to track evolving semantic intent, ensuring that retrieval remains aligned with current stream content and user objectives. While we implement continuous RAG using a *cts_filter* in our figures, a *cts_topk* implementation is equally possible.

Implementation. To illustrate the behavior of our continuous retrieval variants, consider a streaming analytics task where we monitor a user’s stock portfolio. The system maintains a reference table containing the user’s positions—e.g., NVDA, AAPL, MSFT—along with metadata such as percentage allocation, descriptions, and analyst ratings. As news arrives in the stream, the retrieval operator must continuously surface items relevant to these holdings. We implement four variants of the continuous retrieval operator that differ in how prompts and embeddings are maintained. (1) *UP-LLM* maintains a single persistent retrieval prompt, which adapts over time as the portfolio evolves. For example, the operator repeatedly issues a unified query such as “Find recent news that impacts my *stock_portfolio*”, allowing the LLM to internally adjust its scope as holdings change (e.g., adding or removing NVDA or AAPL). (2) *SP-LLM* uses multiple LLM-generated sub-prompts to track finer-grained intents. Under the portfolio example, *SP-LLM* creates separate sub-prompts such as “Find news about NVDA”, “Find news about AAPL”, and “Find news about MSFT”, ensuring more precise and entity-aligned retrieval. (3) *UP-Emb* mirrors the unified strategy of *UP-LLM* but performs retrieval in embedding space: both the unified prompt and news items are embedded and matched through vector similarity search. (4) *SP-Emb* combines sub-prompting with embedding-based retrieval: each symbol-specific prompt (e.g., NVDA, AAPL, MSFT) is encoded as a vector query, enabling specialized, scalable matching across high-volume news streams.

Evaluation. We conduct two experiments. (1) On MiDe22 [21], we compare all four *continuous filter* variants across three topical categories (Ukraine, COVID-19, Refugees), reporting both F1 and throughput. (2) On FNSPID [7]—a financial news dataset with aligned stock-price information for all S&P 500 companies. We select 10 companies and vary the number of monitored companies (i.e., number of predicates or sub-prompts) from 2 to 10, reporting

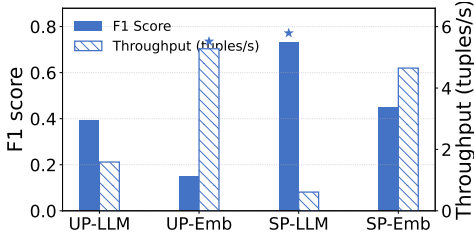


Figure 4: Continuous RAG implementations on the MiDe22 dataset

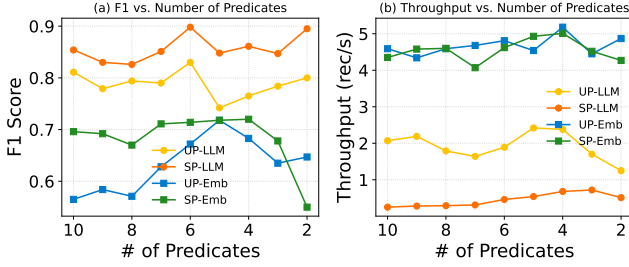


Figure 5: Continuous RAG under varying predicate counts (2–10). Left: F1 versus # predicates. Right: throughput (rec/s) versus # predicates.

F1 and throughput to test whether the trends remain consistent under differing predicate counts.

Takeaway. Figure 4 reports performance across the four variants of continuous filtering. As expected, SP-LLM achieves the highest F1 because it leverages full LLM reasoning and decomposes the predicate set into semantically focused subprompts. Conversely, UP-Emb delivers the highest throughput, reflecting the efficiency of unified prompting combined with lightweight embedding-based retrieval. To further validate these assumptions, we vary the number of predicates and examine how accuracy and throughput scale with predicate complexity.

Figure 5 summarizes the trends as the number of predicates increases. We note two observations: (i) SP-LLM consistently yields the highest F1 across predicate counts, reflecting superior semantic tracking as intent granularity increases. In contrast, UP-LLM experiences mild accuracy degradation, consistent with instruction interference when multiple predicates are fused into a single prompt. (ii) UP-Emb and SP-Emb maintain high, stable throughput across scales, demonstrating resilience to predicate growth, while LLM-based variants show slower but more adaptive reasoning. Overall, the results show that prompt factorization (SP) improves accuracy under increasing predicate complexity, whereas embedding-based retrieval preserves throughput scalability.

4 OPTIMIZATIONS

This section presents two key streaming-specific operator-level optimizations that improve the throughput of LLM-powered stream processing: *tuple batching* and *operator fusion*. Although both methods can substantially increase throughput, they entail intrinsic

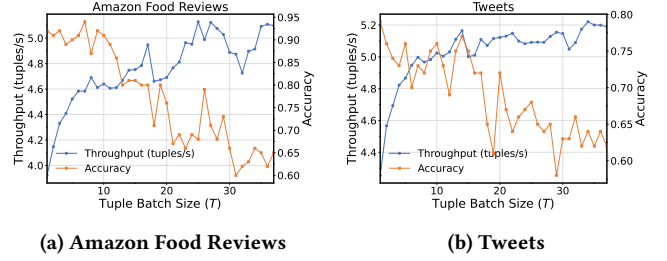


Figure 6: Tuple batching sensitivities for single operators on short (Twitter) and longer (Amazon Fine Food Reviews) texts.

trade-offs: gains in efficiency commonly come at the cost of reduced accuracy or diminished semantic fidelity.

4.1 Tuple Batching

Tuple batching processes multiple input tuples within a single LLM call, amortizing invocation cost and token usage across several data items and thereby reducing the number of model calls. However, batching introduces a trade-off: as more tuples are aggregated into a single prompt, the prompt grows longer and more complex, which can lead to quality loss if the model struggles to handle multiple inputs simultaneously. While recent work on *batch prompting* [5] has explored joint processing of multiple inputs to improve LLM inference efficiency, these techniques have not been studied in the context of *semantic relational pipelines*. Our work examines tuple batching as an operator-level optimization inside continuous, stateful LLM pipelines, studying how batching interacts with semantic operators, affects downstream accuracy, and contributes to end-to-end throughput in streaming settings.

Implementation. We implement tuple batching by explicitly restructuring prompts to maximize their shared prefix and minimize redundant tokens across tuples. Given a batch of T input tuples, each operator starts from a logical per-tuple prompt template consisting of: (i) a system prompt describing the role of the model, (ii) an instruction prompt describing the task, and (iii) an output schema specification. Instead of issuing T independent LLM calls, we construct a single batched prompt as follows:

- (1) *Shared prefix construction:* We move all shared content, including the system prompt, task description, and schema, to the beginning of the prompt, forming a common prefix that can be reused across the entire batch.
- (2) *Tuple enumeration:* We append the input stream tuples as numbered items, each labeled with a stable tuple identifier.
- (3) *Output specification:* We ask the model to return a JSON list whose j -th entry corresponds to the input tuple j , so that outputs can be deterministically mapped back to the original tuples.

Evaluation. We evaluate how tuple batching balances efficiency and accuracy, and characterize each operator’s *batching sensitivity*—its performance response to varying batch size T and input length. Using the `sem_map` sentiment classification operator, we compare two datasets with contrasting input lengths—short Twitter texts [6] and longer Amazon Fine Food Reviews [15]—to quantify how throughput and accuracy evolve as T increases. Figure 6 illustrates the resulting throughput–accuracy trade-offs and highlights the differing sensitivities of operators to batching.

Table 2: Operators, tasks, and evaluation metrics used in the stock news dataset.

Operator	Task	Metric
map _{bi}	Binary sentiment classification (<i>positive</i> vs. <i>negative</i>)	F1
map _{multi}	Multi-class classification extracting the referenced company (e.g., AAPL, TSLA)	Macro-F1
map _{sum}	Sentence-level summarization of a single news item	BERTScore-F1
filter	Boolean semantic filter that keeps tuples referring to a target company	F1
topk _k	Selects the k most impactful news items ($k = 1, 3, 9$)	Recall@k
agg	Window-level summarization of news content and sentiment	BERTScore-F1
E2E Pipeline	All operators jointly	F1

4.2 Operator Fusion

Operator fusion [22] executes multiple logical operators within a single LLM invocation by combining adjacent operators to eliminate redundant prefill and per-request overhead. Rather than invoking the model separately for each stage (e.g., *filter*, *map*), fusion composes consecutive operators into one prompt, thereby reducing repeated initialization costs and token-level computation. A key potential side effect is *semantic interference*, where combining multiple operator intents into a single prompt can alter or degrade model behavior unless the prompt is carefully structured and validated.

Implementation. To execute a chain of operators in a single LLM call, VectraFlow constructs a *fused schema* that exposes all fields produced across the sequence. For a fusible chain $\Pi = (op_1, \dots, op_L)$, the fused schema is defined as

$$\text{schema}(\text{fuse}(\Pi)) = \text{schema}(op_1) \cup \dots \cup \text{schema}(op_L),$$

with attribute name collisions resolved through namespacing or user-defined aliases. The LLM is then instructed, via a fused prompt, to apply each operator’s logic step-by-step and output a single JSON object adhering to the combined schema, thereby preserving the pipeline’s semantics within one invocation.

Evaluation. We evaluate the operator fusion on a curated FN-SPID [7] subset and report execution time (s), accuracy at both operator and end-to-end (E2E) levels, and token usage (prompt/prefill vs. generation). All stages use gpt-4o-mini. VectraFlow exposes a comprehensive set of semantic operators and their fusible combinations, and we evaluate both individual operators and all valid fused variants. To capture a range of task difficulties, we run each operator on multiple settings (e.g., binary classification, multi-class classification, and summarization for *map*). Table 2 summarizes each operator, its task, and the evaluation metrics.

Filter-Aware Fusion. A filter behaves like a binary map whose selectivity controls downstream load, so we evaluate it separately. Table 3 compares unfused vs. fused orders for *map* and *filter*: fusing yields $\sim 1.31\times$ speedup for *map* \rightarrow *filter* and $\sim 1.08\times$ for *filter* \rightarrow *map*, with accuracy drops of 0.065 and 0.047, respectively.

We vary filter selectivity s in Table 4 and observe that low selectivity (dropping most tuples) makes fusion worse, since the fused pipeline still executes the downstream operator on tuples the filter

Table 3: Filter-involved fusion: time, accuracy, and token usage. Tokens reported as P/G = prompt / generation.

Approach	Time (s)	Accuracy	Operator	Tokens (P/G)
Map \rightarrow Filter	52.12	0.780	Map Filter	225/27 218/10
Fused (Map \rightarrow Filter)	39.76	0.715	Fused Op	324/33
Filter \rightarrow Map	42.83	0.791	Filter Map	220/10 240/28
Fused (Filter \rightarrow Map)	39.64	0.744	Fused Op	324/33

Table 4: Relative speed gain of Fused vs. Non-Fused under filter selectivity s .

Fusion Type	10%	30%	50%	80%	100%
Map \rightarrow Filter (Fused vs. Non-Fused)	23.11%	23.40%	21.72%	21.16%	19.43%
Filter \rightarrow Map (Fused vs. Non-Fused)	-10.35%	-3.99%	3.21%	16.27%	21.17%

would have discarded, outweighing the benefits of eliminating an extra call. As s increases, this penalty shrinks and the benefit of eliminating an extra LLM call grows, making fusion increasingly favorable and eventually dominant.

Filter-Free fusion. Table 5 reports fusion outcomes for non-filter operator pairs using the formal operator labels. Each row pair shows the baseline pipeline and its fused counterpart, along with the measured *Speedup*, *F1 loss*. As a rule of thumb, smaller $|\Delta|$ (trade-off ratio closer to 0) indicates a more favorable performance–accuracy balance.

Takeaway. These results suggest a rule of thumb for when fusion is effective. Fusion is generally safe and beneficial for operator pairs that apply lightweight transformations. This includes *map* \rightarrow *map*, *op* \rightarrow *map*, and *op* \rightarrow *filter*, where we observe low sensitivity and a trade-off ratio (Δ) close to zero. Fusion becomes more fragile for operators such as *topk* and *agg*, where the output depends heavily on ranking quality or the reliability of the generated summary. In these cases, accuracy is more sensitive to small LLM errors, and speedups depend on parameters such as k or window size. When k approaches the window size, the operator effectively selects all elements in the window, accuracy increases because the operator no longer relies on fine-grained ranking. Fusion can be risky for *topk* and *agg*, as its stability still depends on k , and should therefore be validated empirically. Fusion is most effective when operators apply light transformations and least stable when they require precise ranking or summarization behavior.

5 DYNAMIC PLANNING FRAMEWORK

Our dynamic planning framework (Figure 7) comprises three components: a *plan generator*, which enumerates candidate configurations (batch sizes, operator variants, and fusion options); a *cost estimator*, which learns per-operator throughput and accuracy models from sampled configurations; and a *plan optimizer*, which uses these models to predict pipeline-level performance, construct the Pareto frontier, and select the configuration that meets user-specified throughput and accuracy targets.

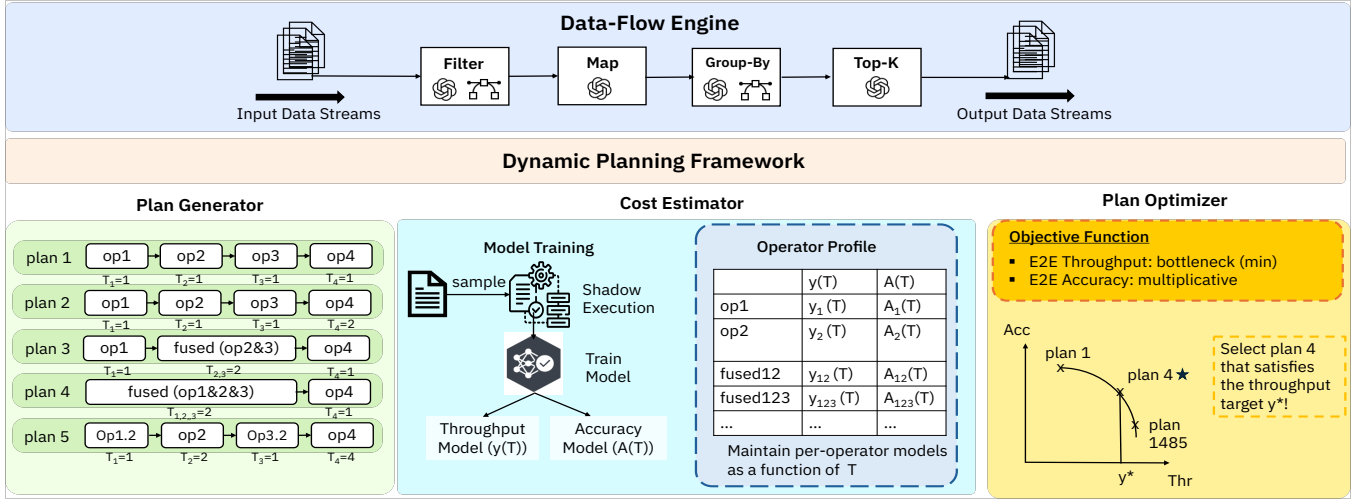


Figure 7: Overview of the dynamic planning framework in VectraFlow.

Table 5: Baseline vs. fused operator performance with throughput speedup and F1 loss. A smaller $\Delta(\text{F1 loss})/\Delta(\text{speedup})$ indicates a better throughput-accuracy tradeoff. Values marked with * denote better throughput-accuracy tradeoffs (smaller $\Delta\text{F1}/\Delta\text{Speedup}$).

Operator Pair	Throughput (base / fused)	E2E F1 (base / fused)	$\Delta\text{F1}/\Delta\text{Speedup}$
map_multi→map_bi	0.65 / 1.13	0.7952 / 0.7730	0.038*
map_bi→map_multi	0.76 / 1.22	0.7879 / 0.7730	0.031*
map_sum→map_bi	0.51 / 0.62	0.6413 / 0.6237	0.130
map_bi→map_sum	0.51 / 0.71	0.6360 / 0.6296	0.027*
map→topk(k=3)	0.87 / 1.48	0.5386 / 0.5238	0.039*
map→topk(k=9)	0.82 / 1.00	0.7867 / 0.7325	0.308
map→agg	0.92 / 3.37	0.7280 / 0.0530	0.344
agg→map	1.02 / 2.49	0.8340 / 0.6530	0.173
topk(k=3)→map	1.13 / 1.31	0.6430 / 0.5430	0.943
topk(k=3)→agg	1.04 / 5.11	0.5900 / 0.3550	0.102
topk(k=3)→topk(k=1)	1.18 / 1.32	0.2860 / 0.2860	0.000*
topk(k=9)→map	0.63 / 1.09	0.9080 / 0.9010	0.011*
topk(k=9)→agg	0.96 / 3.35	0.6020 / 0.5760	0.022*
topk(k=9)→topk(k=1)	0.67 / 1.27	0.5260 / 0.5260	0.000*

5.1 Plan Generation and Pruning

Rather than relying solely on heuristics, VectraFlow collects execution logs from *shadow runs* across the design space to train predictive performance models. To explore this space, the system employs a *plan generator* that automatically enumerates possible execution strategies for a given pipeline. The generator considers four families of plans: (1) a baseline plan without optimizations, (2) fusion plans that combine consecutive operators to reduce invocation and prefill overhead, (3) batching plans that assign different tuple batch sizes to operators to balance throughput and accuracy, and (4) hybrid plans that integrate both fusion and batching. Beyond these optimization strategies, the generator also explores alternative implementations of *continuous semantic operators*, evaluating both LLM-based (prompt-driven) and embedding-based variants to capture different accuracy-throughput trade-offs. It supports

pipelines of arbitrary length and enumerates all feasible combinations up to a configurable maximum batch size, before applying pruning rules to remove invalid or redundant configurations.

The plan generator prunes invalid configurations in the following order: (1) Fusion infeasibility: remove plans that attempt to fuse operators tied to different window contexts, since such operators cannot be fused without contaminating the prompt context. (2) Window constraints: discard plans where the batch size exceeds the active window size ($T > W$), as a batch cannot contain more tuples than the window admits. (3) Batching constraints: enforce non-decreasing batch sizes across consecutive operators ($b_{i+1} \geq b_i$) to maintain balanced throughput, while allowing exceptions for selective operators (e.g., filters), where downstream batch sizes may shrink according to the operator’s selectivity s . Together, these pruning rules substantially reduce the search space while preserving semantically valid and executable plans.

5.2 Cost-Aware Estimation

The planner builds *per-operator* predictive models by sampling data and plan configurations for each operator implementation or variant. For every operator, we collect measurements across different tuple-batch sizes T and train paired models that capture how *throughput* and *accuracy* behave as functions of T . The *throughput model* describes how performance scales with batching, while the *accuracy model* characterizes how quality changes as multiple tuples are processed together.

Throughput Model. Tuple batching affects throughput by increasing the size of the prompt and generated text in proportion to the batch size. Processing a batch of T tuples requires constructing a prompt that embeds all T items (linear in T) and generating T corresponding outputs (also linear in T). Thus, the batch service time for an operator can be well-approximated by an affine function

$$s(T) = aT + b,$$

where a captures the per-tuple inference cost and b reflects fixed overhead such as boilerplate prompt text and model invocation

latency. The resulting per-operator throughput is

$$y(T) = \frac{T}{s(T)} = \frac{T}{aT + b} \quad \text{tuple/s.} \quad (1)$$

This equation expresses an expected trade-off: throughput increases rapidly for small T as fixed overhead is amortized, but gradually saturates as the linear per-tuple cost becomes dominant. This model matches the observed behavior across LLM-based operators, providing a simple, operator-level predictor of batching efficiency.

Accuracy Model. To understand how tuple batching affects operator quality, we evaluate four representative semantic operators drawn from two datasets. From the stock news dataset, we study (i) a *semantic group-by* operator that implements a company classifier, and (ii) a *semantic filter* that implements sentiment analysis. From the Amazon Food Reviews dataset, we evaluate (iii) a *semantic map* operator that summarizes user reviews and (iv) a *semantic top-k* operator that rates the helpfulness of reviews. For each operator, we sweep over a range of batch sizes T and run five trials with different random seeds (1–5) to expose ordering and position effects. This allows us to quantify how batching influences accuracy as more tuples are packed into a single prompt.

In Figure 8, we observe that the same pattern emerges across all operators: accuracy is highest at $T=1$ and then consistently decreases as T grows. The decline is steep for small increases in T and becomes progressively shallower at larger batch sizes. This behavior suggests an *exponential decay* trend, which captures this fast-initial-drop and slow-tail dynamic. Intuitively, batching introduces several sources of degradation, including semantic interference across items, position bias, and reduced attention allocated to any single tuple, which accumulate quickly at first and then taper off as prompts become saturated. We model the expected accuracy at batch size T as

$$A(T) = A_{\max} \cdot e^{-\beta(T-1)}. \quad (2)$$

where A_{\max} corresponds to the operator’s baseline accuracy at $T = 1$ and β is a decay parameter estimated from profiling runs. This formulation aligns with findings from batch prompting studies [5, 10], which report that batching improves efficiency but can degrade model performance due to order sensitivity and cross-item interference. Our exponential model provides a lightweight, empirically grounded approximation of these trends, allowing the planner to predict accuracy loss when exploring batching configurations.

5.3 Plan Optimizer

With per-operator models in place, the optimizer composes these estimates into pipeline-level predictions and recommends plan configurations that best satisfy user-defined throughput and accuracy objectives. Given operator-level throughput $y_i(T)$ and accuracy $A_i(T)$ learned from profiling, the optimizer explores candidate plans, predicts their end-to-end (E2E) performance, constructs the Pareto frontier, and returns a configuration that matches the user’s desired trade-off.

End-to-End Throughput. VectraFlow supports two execution modes, each inducing a different composition rule for end-to-end throughput $y_{e2e}(x)$.

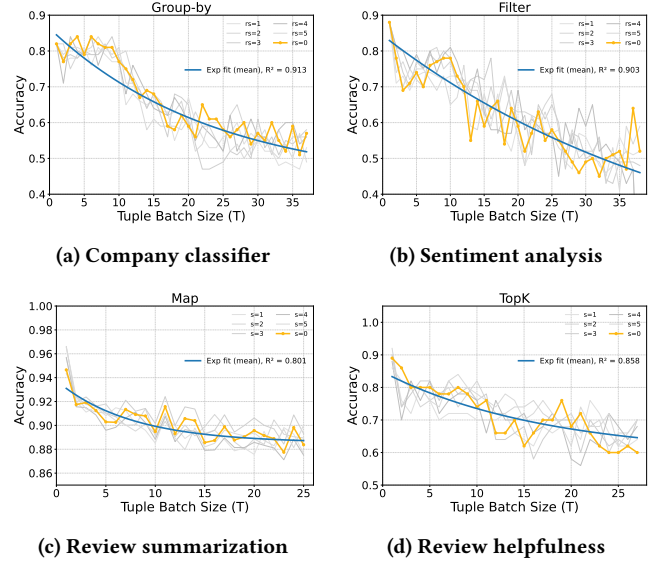


Figure 8: Effect of tuple batch size T on operator accuracy across four operators: (a) company classifier, (b) sentiment analysis, (c) review summarization, and (d) review helpfulness top-k.

Pipeline-parallel execution. When operators run concurrently with multiple in-flight batches, throughput is governed by the bottleneck stage:

$$y_{e2e}(x) = \min_i y_i(T_i).$$

Sequential execution. When batches are processed one at a time, operator latencies accumulate. The corresponding end-to-end throughput is the harmonic mean of operator throughputs:

$$y_{e2e}(x) = \frac{1}{\sum_i 1/y_i(T_i)}.$$

These formulations allow users to select the throughput objective that best matches their execution semantics, or to specify custom alternatives, as long as the objective can be expressed as a function of per-operator throughput (e.g., weighted throughput). Objectives that require joint modeling beyond individual operators are not supported, since VectraFlow maintains learned performance models at the operator level rather than for the entire pipeline.

End-to-End Accuracy. To estimate pipeline-level accuracy, VectraFlow assumes that operators are independent. Under this simplifying assumption, the E2E accuracy for a plan T is approximated as the product of per-operator accuracies:

$$A_{E2E}(T) \approx \prod_i A_i(T_i).$$

The system also supports user-defined accuracy objectives that can be expressed through per-operator models (e.g., weighted products, max/min). For more complex end-to-end metrics (e.g., F1), VectraFlow can fall back to sparse pipeline-level sampling, using those samples as targets for plan selection. Objectives that depend on information unavailable from either operator models or pipeline outputs are out of the scope of our current framework.

Plan Selection and Pareto Frontier. For each candidate plan, the optimizer evaluates the chosen throughput metric together with its predicted E2E accuracy, constructs the Pareto frontier of non-dominated plans, and then returns a configuration that either meets a user-specified throughput target with the highest possible accuracy or provides the best accuracy–performance trade-off along the frontier. This approach allows the optimizer to efficiently navigate a large plan space and tailor recommendations to the unique constraints and objectives of each pipeline.

5.4 Extensibility and Modular Optimization

VectraFlow’s optimization framework is modular and extensible by design. Rather than being tied to a fixed set of strategies, it allows new optimization dimensions to be incorporated through lightweight implementation rules. Beyond batching, fusion and alternative operator implementations (LLM-based or embedding-based), the planner can integrate additional layers such as model selection (e.g., switching between lightweight and high-fidelity LLMs) or query rewriting. Each module exposes a uniform interface, enabling the planner to reason jointly about model capacity, operator fidelity, and resource usage. This design allows VectraFlow to remain adaptable and to incorporate future inference and optimization techniques without modifying the core planning logic.

6 MULTI-OBJECTIVE BAYESIAN OPTIMIZATION

Learning the throughput–accuracy Pareto frontier of an LLM-based pipeline requires selectively probing operators under different tuple batch sizes T and sampling rates s . Exhaustive enumeration is infeasible: even a four-operator pipeline with $T \leq 10$ already yields over 20,000 plan configurations. Since we can only sample a small subset of operators and configurations, the key challenge is deciding *which* operators to probe and *at what* sampling rates. This motivates a *Cost-Aware Multi-Objective Bayesian Optimization* (MOBO) framework that leverages structural priors—such as the monotonic and saturating relationships between batching, throughput, and accuracy to guide exploration. By encoding these operator-level trends as prior functions, MOBO learns the Pareto frontier far more efficiently than naive random or bandit-based sampling, enabling principled allocation of a limited probing budget.

6.1 Problem Statement

We aim to learn the throughput–accuracy Pareto frontier of a multi-operator LLM pipeline under a fixed probing cost budget B . Each probe evaluates a configuration (i, T, s) —operator index, tuple batch size, and sampling rate—and consumes part of this budget. The goal is to discover high-quality pipeline plans that differ in batching choices, fusion decisions, and operator variants while respecting the total probing budget. Formally, we solve the multi-objective optimization problem

$$\max_{x \in \mathcal{X}} (y_{e2e}(x), A_{e2e}(x)) \quad \text{s.t.} \quad \sum_{t=1}^N \text{cost}(i_t, T_t, s_t) \leq B,$$

where \mathcal{X} is the space of all feasible plan configurations, $y_{e2e}(x)$ denotes end-to-end throughput, and $A_{e2e}(x)$ denotes end-to-end accuracy. The goal is to recover the Pareto-optimal set.

6.2 Algorithm

Phase I: Model Warm-Up and Priors. We begin with a lightweight warm-up phase using a small sampling rate (e.g., $s_0=0.1$). Each operator is probed at a few representative batch sizes (e.g., $T \in \{1, 2, 8\}$), producing initial measurements that seed the surrogate models. From these warm-up samples, we fit two parametric priors that capture the empirical behavior described in Section 5.2: the throughput prior (Eq. 1) and the accuracy prior (Eq. 2). These priors reflect the observed sublinear saturation of throughput with batch size and the exponential decay of accuracy as more tuples share a prompt.

Using these priors, each operator maintains two independent Gaussian-process (GP) surrogate models—for throughput and accuracy—with mean functions $\mu_{y_i}(T)$ and $\mu_{A_i}(T)$ and predictive variances $\sigma_{y_i}^2(T)$ and $\sigma_{A_i}^2(T)$. To model the effect of sampling rate s , we augment the GP observation noise with a variance term proportional to $1/s$, reflecting that lower sampling rates yield noisier estimates. We treat operators as conditionally independent given the GPs. For any plan configuration x , we obtain a predictive distribution over end-to-end throughput and accuracy by composing the operator-level predictive Gaussians according to the user-specified pipeline objective (e.g., bottleneck throughput and multiplicative accuracy).

Phase II: Cost-Aware Acquisition and Iterative Probing. We select the next probe by maximizing a cost-aware acquisition function:

$$U(i, T, s) = \frac{\text{EHVI}(i, T, s)}{\text{cost}(i, T, s)}, \quad (i^*, T^*, s^*) = \arg \max_{i, T, s} U(i, T, s).$$

Expected Hypervolume Improvement (EHVI). Let \mathcal{F} be the current non-dominated frontier and r a dominated reference point. For a probe that updates operator i at (T, s) , we compute

$$\text{EHVI}(i, T, s) = \mathbb{E}[\text{HVI}((y_{e2e}, A_{e2e}), \mathcal{F}; r)],$$

using a Gaussian approximation to the predictive distribution from operator-level surrogates (with the expectation evaluated via Monte Carlo). End-to-end predictions are obtained by composing the per-operator surrogate posterior means according to the user-specified objectives. By default, we use bottleneck throughput $y_{e2e}(x) = \min_i y_i(T_i)$ and multiplicative accuracy $A_{e2e}(x) = \prod_i A_i(T_i)$.

Cost model. We approximate the cost of probing a configuration (i, T, s) as

$$\text{cost}(i, T, s) = \frac{ns}{\hat{y}_i(T)}.$$

where n is the number of tuples used for profiling, s is the sampling rate, ns denotes the number of tuples actually processed during the probe, $\hat{y}_i(T)$ denotes the posterior mean of the throughput surrogate, yielding a simple and adaptive estimate of the probe’s execution time.

After selecting a probe (i^*, T^*, s^*) , we execute it to obtain the observed throughput and accuracy, update the corresponding operator-level Gaussian surrogates, and refresh the non-dominated frontier \mathcal{F} using the updated end-to-end predictions. This cycle continues until the probing budget B is exhausted, at which point we evaluate all explored configurations under the final surrogate means and extract pipeline’s resulting throughput–accuracy Pareto frontier.

7 EVALUATION

We evaluate VectraFlow on two representative streaming pipelines to examine two key experimental claims:

- **Effectiveness of optimization strategies.** We show that both operator-level and pipeline-level optimizations, including tuple batching and operator fusion, can substantially improve performance, while the planner selects configurations that minimize accuracy degradation for the desired throughput level.
- **Sampling efficiency through MOBO.** We show that cost-aware sampling strategies, guided by multi-objective Bayesian optimization, allow VectraFlow to identify Pareto-efficient plans more efficiently than heuristic or random baselines.

7.1 Experimental Setup

To evaluate the performance characteristics of our proposed techniques within the VectraFlow system, we conducted a series of experiments. We evaluate our techniques using the Qwen/Qwen2.5-7B-Instruct model, a 7B-parameter instruction-tuned language model capable of handling complex, structured prompts. The model is deployed using the vLLM [9] inference server, which provides efficient batching and prefix caching. All experiments are conducted on a single NVIDIA GeForce RTX 3090 GPU with 24GB of memory. For reproducibility, we set temperature to $t = 0$ for all methods and baselines, unless otherwise stated. This setup reflects a realistic production-grade inference stack for streaming LLM applications.

We evaluate our dynamic planning framework in an *offline* setting using a train-test split of 100 data points each: 100 data points are used to train the throughput and accuracy models, and another 100 are used to evaluate how well each method recovers the ground-truth frontier. A larger training set is impractical because the plan space exceeds 10,000 configurations, and fully evaluating all of them requires more than 48 hours of end-to-end execution time. Each method is then run on this offline workload and produces its own predicted Pareto-optimal plans under a given budget, enabling a direct comparison between the predicted and actual frontiers. In practice, this offline frontier also enables online adaptation: at runtime, the system maps the observed arrival rate to the corresponding point on the precomputed frontier and selects the optimal plan configuration.

We compare four strategies: (1) *Heuristic-Guided Sampling Per-Pipeline (Heuristic Pipe)*, which evaluates full pipeline configurations using rule-driven heuristics derived from a small warm-up phase; (2) *Heuristic-Guided Sampling Per-Operator (Heuristic Op)*, which applies the same heuristics but samples operator configurations independently; (3) *MOBO (no warmup)*, our multi-objective Bayesian optimization framework without the warm-up stage; and (4) *MOBO*, which incorporates warm-up and prior-guided exploration. Both heuristic-guided methods use statistics collected during the warm-up phase to identify unpromising plans (e.g., fuse operators 1 and 2), enabling the sampler to prune the search space before evaluation. We also evaluated *Random Sampling Per-Pipeline* (Random Pipe) and *Random Sampling Per-Operator* (Random Op), but as both methods were consistently inferior to the heuristic-guided strategies, we omit them from the subsequent results for clarity.

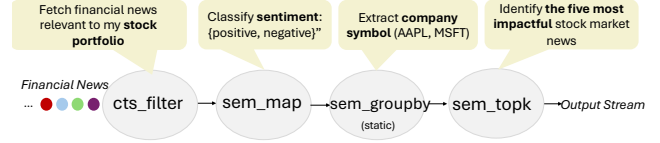
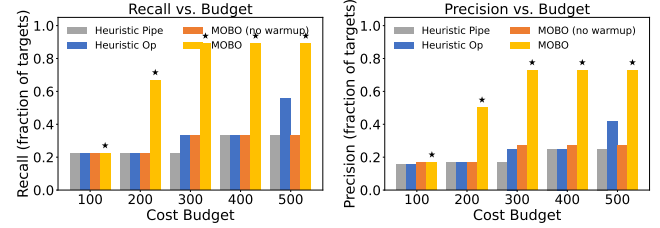


Figure 9: Stock News Monitoring Pipeline.



(a) Recall vs. Cost Budget.

(b) Precision vs. Cost Budget.

Figure 10: Recall and Precision vs. Cost Budget for the Stock News Monitoring Pipeline. MOBO consistently achieves higher recall and precision across all budgets, saturating after $B=300$ as it recovers nearly all Pareto-optimal plans.

7.2 Stock News Monitoring

Pipeline. Figure 9 shows our semantic streaming pipeline for stock monitoring on the FNSPID [7] dataset. A live financial news feed is first processed by the `cts_filter` operator, which continuously retrieves and filters news articles relevant to a given stock portfolio. The filtered stream is passed to a `sem_map`, which performs data cleaning and structuring to normalize the input. Next, a `sem_groupby` groups news articles by their associated company ticker (e.g., TSLA, AAPL). Within each group, the `sem_topk` operator selects the most impactful articles using a `sem_window` that adapts to topic drift in financial news, ensuring that related developments are grouped together even when they unfold gradually across multiple articles. Finally, `sem_agg` summarizes the top-ranked articles within a count-based window, producing concise portfolio-level insights and recommendations.

Results. Figure 10 reports recall and precision under fixed cost budgets (B), measuring how many true Pareto frontier plans each method successfully retrieves. Across all budgets, MOBO consistently achieves the highest recall, converging near $B=300$ with diminishing improvements thereafter. Heuristic Op outperforms Heuristic Pipe because full-pipeline evaluation wastes budget on end-to-end measurements, whereas operator-level sampling allows more focused exploration. The MOBO variant without warmup retrieves fewer frontier plans, showing that the warm-up phase is key for stabilizing early model behavior and speeding up convergence.

Table 6 summarizes the prevalence of execution optimizations among Pareto-efficient plans at $B=300$. Across all retrieved plans, both tuple batching and operator fusion appear frequently. In particular, batching dominates across nearly all efficient pipelines, while fusion appears more selectively.

Figure 11 shows a stepwise adoption of execution optimizations along the Pareto frontier. Early gains come solely from tuple batching, which preserves high accuracy; higher-throughput regions

Table 6: Adoption of execution optimizations across Pareto-efficient plans for the Stock News Monitoring Pipeline.

Optimization Type	Pipeline-Level	Operator-Level
Tuple Batching	8 / 9 (89%)	16 / 36 (44%)
Operator Fusion	3 / 9 (33%)	6 / 36 (17%)
Operator Variants	0 / 9 (0%)	0 / 36 (0%)

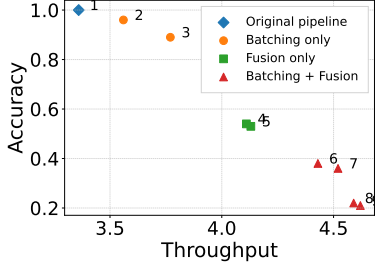


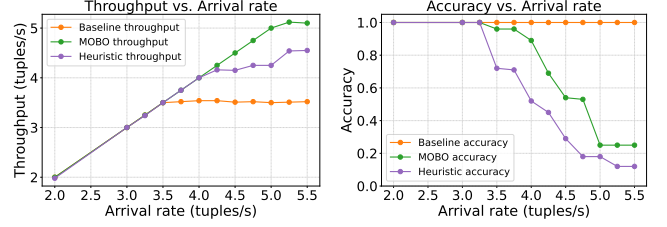
Figure 11: Stepwise adoption of optimization strategies along the Pareto frontier for the Stock News Monitoring Pipeline.

introduce fusion for additional speedup; and the extreme end combines batching and fusion to maximize throughput at the cost of modest accuracy loss. This progression illustrates how VectraFlow adaptively selects optimizations across throughput tiers. No filter variants appear among these efficient plans because the optimization objective was defined on *bottleneck throughput*: while embedding-based filters increase total throughput, they marginally reduce accuracy and do not improve the slowest stage in the pipeline.

Figure 12 reports throughput and accuracy as we simulate a streaming workload by replaying 1,200 tuples with Poisson inter-arrival times. The arrival rate λ increases every 100 tuples, progressively stressing the system. In the throughput plot (Figure 12a), the *baseline* shows an almost flat curve: because its plan is fixed, it cannot react to higher arrival rates. In contrast, *MOBO* dynamically reconfigures the pipeline as λ increases, allowing its throughput to closely track—and eventually saturate at—the system’s maximum achievable rate after leveraging all available execution optimizations (tuple batching, fusion, and operator variants). The *heuristic* strategy initially keeps up, but saturates much earlier and steadily falls behind as the stream accelerates. In the accuracy plot (Figure 12b), the *baseline* maintains perfect accuracy because it never changes configuration. The *heuristic* policy suffers the steepest drop: its aggressive reconfigurations fail to meet throughput demands while substantially degrading accuracy. *MOBO* also trades accuracy for speed at high arrival rates, but does so in a controlled, model-guided manner, preserving significantly more accuracy than the heuristic in the overloaded regime.

7.3 Misinformation Event Monitoring

Pipeline. Figure 13 illustrates our end-to-end semantic streaming pipeline for misinformation event monitoring. We continuously ingest the MiDe22 stream, apply a `sem_filter` to discard items unlikely to contain misinformation, dynamically group the remaining tuples by semantic topic via `sem_groupby`, segment each topic’s flow into dynamic event-context windows using `sem_window`, and



(a) Throughput vs. Arrival Rate. (b) Accuracy vs. Arrival Rate.

Figure 12: Throughput and Accuracy vs. Arrival Rate for the Stock News Monitoring Pipeline.

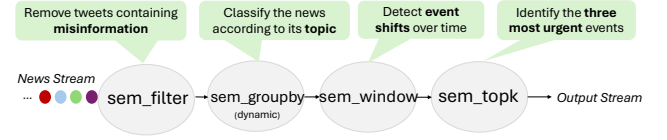
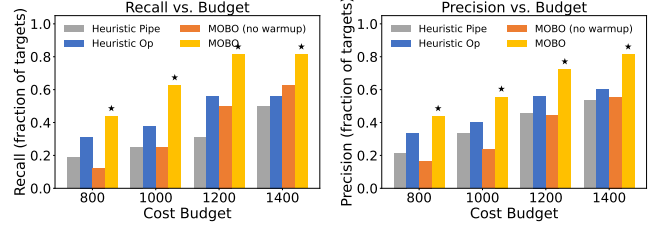


Figure 13: Misinformation Event Monitoring Pipeline.



(a) Recall vs. Cost Budget (b) Precision vs. Cost Budget

Figure 14: Recall and Precision vs. Cost Budget for the Misinformation Event Monitoring Pipeline. MOBO maintains superior recall and precision, yielding higher-quality retrievals than random baselines.

within every window compute `sem_topk` ($k = 3$) based on an urgency scoring function. The pipeline produces a live feed of the three most urgent misinformation events per window for downstream alerting, monitoring, or visualization.

Results. Figure 14 reports recall and precision under fixed cost budgets ($B = \{800, 1000, 1200, 1400\}$), measuring how many true-Pareto frontier plans each method successfully retrieves. MOBO consistently achieves the highest recall and precision, converging near $B=1200$ with diminishing improvements thereafter. Heuristic Op consistently surpasses Heuristic Pipe because Pipe allocates its budget to complete end-to-end evaluations instead of focused operator-level probes. The MOBO variant without warmup retrieves fewer frontier plans, underscoring the importance of the warmup phase for stabilizing initial model behavior and speeding up convergence.

Table 7 shows that tuple batching is universally adopted across all efficient pipelines (excluding the baseline) and thus serves as the primary throughput optimization. Operator variants are also present in every pipeline, with most pipelines relying on embedding-based variants. In contrast, operator fusion appears only once, suggesting that it offers benefits only in a narrow set of high-throughput cases and is not broadly advantageous across the Pareto frontier.

Table 7: Adoption of execution optimizations across Pareto-efficient plans for the Misinformation Event Monitoring Pipeline.

Optimization Type	Pipeline-Level	Operator-Level
Tuple Batching	15 / 16 (94%)	48 / 64 (75%)
Operator Fusion	1 / 16 (6%)	2 / 64 (3%)
Operator Variants	15 / 16 (94%)	64 / 64 (100%)
sem_groupby (embedding)	7 / 16 (44%)	28 / 64 (44%)
sem_window (pairwise)	4 / 16 (25%)	16 / 64 (25%)
sem_window (clustering)	4 / 16 (25%)	16 / 64 (25%)

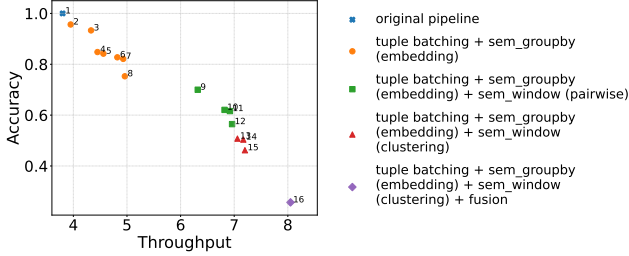


Figure 15: Stepwise adoption of execution optimizations along the Pareto frontier for the Misinformation Event Monitoring Pipeline.

Figure 15 illustrates a clear stepwise adoption of optimizations along the throughput–accuracy frontier. All Pareto-optimal pipelines use tuple batching and `sem_groupby` (embedding) as a baseline, while progressively stronger techniques are added with increasing throughput: mid-range configurations incorporate `sem_window` (pairwise), higher-throughput designs replace this with `sem_window` (clustering), and the maximum-throughput setup additionally applies operator fusion over these variants. This pattern shows that VectraFlow progressively adds execution optimizations to boost throughput, accepting substantial accuracy degradation only in its most aggressive, fusion-driven mode.

8 RELATED WORK

LLM-powered data processing systems and optimizations. A growing line of systems extends the relational model with semantic operators for processing unstructured data using LLMs [2, 8, 11, 13, 17, 19]. Lotus [17] introduces a declarative interface for semantic pipelines and optimizes individual operators via model cascades that combine a high-quality “gold” algorithm with a cheap proxy. Palimpsest [12] and its successor Abacus [18] explore cost-based optimization over models, prompts, and operator variants, formulating pipeline selection as a multi-objective optimization problem in offline, batch settings. DocETL [19] applies LLM-based query rewriting to transform documents into structured representations, using LLMs both to rewrite pipelines and validate the rewrites. ZenDB [11] targets semi-structured document analytics with semantic indexes and logical rewrites such as predicate reordering and projection pull-up. These systems all operate in batch or one-shot modes over static datasets. They do not address the challenges of continuous execution over unbounded, evolving streams, nor do

they model or optimize the runtime performance–accuracy trade-offs that arise when LLM operators must be executed persistently.

Our prior work (VectraFlow [14]) provides the vector-based analogue of a continuous processing engine, supporting streaming operations over embedding vectors. In contrast, this paper brings continuous processing to the LLM layer: we introduce continuous semantic operators, model their accuracy–throughput behavior, and develop a dynamic optimization framework—including tuple batching, operator fusion, embedding-based variants, and MOBO-driven plan selection—for continuous LLM-powered pipelines.

Stream processing systems. Early systems (e.g., Aurora [1], STREAM [16]) established the foundations of modern data-stream management, introducing core techniques for continuous queries, approximation, and adaptive resource management. These ideas were later extended by open-source engines such as Apache Flink [3] and Apache Storm [20], which advanced the field through unified batch/stream execution, low-latency pipelines, and scalable, fault-tolerant processing over structured data streams.

In contrast, VectraFlow targets LLM-based data processing over unstructured streams with novel continuous semantic operators. It integrates LLM-native optimizations into a dynamic planning framework. Whereas conventional systems emphasize standard performance metrics, VectraFlow explicitly incorporates accuracy, allowing for systematic performance–accuracy trade-offs that are intrinsic to LLM-based processing.

9 CONCLUSIONS

This paper introduces *Continuous Prompts*, a new framework for LLM-augmented stream processing that enables persistent, semantic-aware queries over unstructured data. We extended RAG to streaming settings, defined continuous semantic operators with several practical implementations, and characterized LLM-specific execution optimizations that shape the performance–accuracy trade-offs of continuous LLM pipelines. We further developed a dynamic planning framework that models operator sensitivities and uses a multi-objective Bayesian optimization (MOBO) strategy to learn throughput–accuracy frontiers under limited probing budgets.

Our evaluation, combining operator-level microbenchmarks with realistic end-to-end pipelines, shows that continuous prompts can dynamically adapt to workload fluctuations and effectively navigate accuracy–efficiency trade-offs in evolving unstructured streams. Taken together, these contributions advance LLM-based stream processing from static, one-shot pipelines to adaptive, continuously optimized semantic computations over unbounded data.

ACKNOWLEDGMENTS

We gratefully acknowledge the support provided by a Brown Seed Fund. We extend our special thanks to Weili Shi for his major contributions to the initial VectraFlow prototype. We also thank the rest of the team for their valuable feedback throughout this work.

REFERENCES

- [1] D. J. Abadi, D. Carney, U. Çetintemel, M. Cherniack, C. Convey, S. Lee, M. Stonebraker, N. Tatbul, and S. Zdonik. Aurora: A new model and architecture for data stream management. *The VLDB Journal*, 12(2):120–139, 2003. doi: 10.1007/s00778-003-0095-z. URL <https://doi.org/10.1007/s00778-003-0095-z>.
- [2] S. Arora, B. Yang, S. Eyuboglu, A. Narayan, A. Hojel, I. Trummer, and C. Ré. Language models enable simple systems for generating structured views of

- heterogeneous data lakes. *Proceedings of the VLDB Endowment*, 17(P92), 2024. doi: 10.14778/3626292.3626294. URL <https://www.vldb.org/pvldb/vol17/p92-arora.pdf>.
- [3] P. Carbone, A. Katsifodimos, S. Ewen, V. Markl, S. Haridi, and K. Tzoumas. Apache Flink™: Stream and batch processing in a single engine. *Bulletin of the IEEE Computer Society Technical Committee on Data Engineering*, 38(4):28–38, 2015.
 - [4] M. Charikar, C. Chekuri, T. Feder, and R. Motwani. Incremental clustering and dynamic information retrieval. *SIAM Journal on Discrete Mathematics*, 17(2): 237–258, 2003.
 - [5] Z. Cheng, J. Kasai, and T. Yu. Batch prompting: Efficient inference with large language model APIs. In *Proceedings of the 2023 Conference on Empirical Methods in Natural Language Processing: Industry Track*, pages 792–810, Singapore, 2023. Association for Computational Linguistics. doi: 10.18653/v1/2023.emnlp-industry.74. URL <https://aclanthology.org/2023.emnlp-industry.74/>.
 - [6] K. Community. Twitter entity sentiment analysis dataset. <https://www.kaggle.com/datasets/jp797498e/twitter-entity-sentiment-analysis>, 2024.
 - [7] Z. Dong, X. Fan, and Z. Peng. Fnspid: A comprehensive financial news dataset in time series. In *Proceedings of the 30th ACM SIGKDD Conference on Knowledge Discovery and Data Mining (KDD '24)*, pages 4918–4927, 2024. doi: 10.1145/3637528.3671629.
 - [8] O. Khatlab, A. Singhvi, P. Maheshwari, Z. Zhang, K. Santhanam, S. Vardhamanan, S. Haq, A. Sharma, T. T. Joshi, H. Moazam, et al. Dspy: Compiling declarative language model calls into self-improving pipelines. *arXiv preprint arXiv:2310.03714*, 2023.
 - [9] W. Kwon, Z. Li, S. Zhuang, Y. Sheng, L. Zheng, C. H. Yu, J. E. Gonzalez, H. Zhang, and I. Stoica. Efficient memory management for large language model serving with pagedattention. In *Proceedings of the 27th ACM SIGOPS Symposium on Operating Systems Principles (SOSP) '23*, pages 506–522, 2023. doi: 10.1145/3600066.3613165.
 - [10] J. Lin, M. Diesendruck, L. Du, and R. Abraham. Batchprompt: Accomplish more with less. In *International Conference on Learning Representations (ICLR 2024)*. OpenReview.net, 2024. URL https://proceedings.iclr.cc/paper_files/paper/2024/file/5d8c01de2dc698c54201c1c7d0b86974-Paper-Conference.pdf.
 - [11] Y. Lin, M. Hulsebos, R. Ma, S. Shankar, S. Zeighami, A. G. Parameswaran, and E. Wu. Querying templated document collections with large language models. In *41st IEEE International Conference on Data Engineering (ICDE 2025)*, pages 2422–2435. IEEE, 2025. doi: 10.1109/ICDE65448.2025.00183. URL <https://doi.org/10.1109/ICDE65448.2025.00183>.
 - [12] C. Liu, M. Russo, M. Cafarella, L. Cao, P. B. Chen, Z. Chen, M. Franklin, T. Kraska, S. Madden, R. Shahout, and G. Vitagliano. Palimpsest: Optimizing ai-powered analytics with declarative query processing. In *Proceedings of the 15th Conference on Innovative Data Systems Research (CIDR)*, 2025.
 - [13] S. Liu, J. Xu, W. Tjangnaka, S. J. Semnani, C. Yu, and M. S. Lam. Suql: Conversational search over structured and unstructured data with large language models. In *Findings of the Association for Computational Linguistics: NAACL 2024*, pages 4535–4555. Association for Computational Linguistics, June 2024. doi: 10.18653/v1/2024.findings-naacl.283. URL <https://aclanthology.org/2024.findings-naacl.283/>.
 - [14] D. Lu, S. Feng, J. Zhou, F. Solleza, M. Schwarzkopf, and U. Çetintemel. Vectraflow: Integrating vectors into stream processing. In *Proceedings of the 15th Annual Conference on Innovative Data Systems Research (CIDR '25)*, 2025.
 - [15] J. McAuley and J. Leskovec. From amateurs to connoisseurs: Modeling the evolution of user expertise through online reviews. In *Proceedings of the 22nd International Conference on World Wide Web (WWW '13)*, pages 897–908. ACM, 2013. doi: 10.1145/2488388.2488477. URL <https://snap.stanford.edu/data/web-FineFoods.html>.
 - [16] R. Motwani, J. Widom, A. Arasu, B. Babcock, S. Babu, M. Datar, G. S. Manku, C. Olston, J. Rosenstein, and R. Varma. Query processing, approximation, and resource management in a data stream management system. In *Proceedings of the First Biennial Conference on Innovative Data Systems Research (CIDR)*, 2003.
 - [17] L. Patel, S. Jha, M. Pan, H. Gupta, P. Asawa, C. Guestrin, and M. Zaharia. Semantic operators and their optimization: Enabling LLM-powered analytics. *Proceedings of the VLDB Endowment (PVLDB)*, 18(3):4171–4184, 2025. doi: 10.14778/3749646.3749685.
 - [18] M. Russo, S. Sudhir, G. Vitagliano, C. Liu, T. Kraska, S. Madden, and M. Cafarella. Abacus: A cost-based optimizer for semantic operator systems. *arXiv preprint arXiv:2505.14661*, 2025. URL <https://arxiv.org/abs/2505.14661>.
 - [19] S. Shankar, T. Chambers, T. Shah, A. G. Parameswaran, and E. Wu. Docetl: Agentic query rewriting and evaluation for complex document processing. *Proceedings of the VLDB Endowment*, 18(9), 2025. doi: 10.14778/3746405.3746426.
 - [20] The Apache Software Foundation. Apache storm. <https://storm.apache.org/>. Accessed: 2024-08-02.
 - [21] C. Toraman, O. Özcelik, F. Sahinuç, and F. Can. MiDe22: An annotated multi-tweet dataset for misinformation detection. In *Proceedings of the 2024 Joint International Conference on Computational Linguistics, Language Resources and Evaluation (LREC-COLING 2024)*, pages 11283–11295. ELRA and ICCL, 2024. URL <https://aclanthology.org/2024.lrec-main.986>.
 - [22] U. Çetintemel, S. Chen, A. W. Lee, and D. Raghavan. Making prompts first-class citizens for adaptive llm pipelines. In *Proceedings of the 15th Annual Conference on Innovative Data Systems Research (CIDR'25)*, 2025. URL <https://arxiv.org/abs/2508.05012>. To appear.